

NANOCRYSTALLINE Al_2O_3 POWDERS PRODUCED BY LASER INDUCED GAS-PHASE REACTIONS

E. Borsella, S. Botti
ENEA, Area INN, Dip. Sviluppo Tecnologie di Punta, C.R.E. Frascati
P.O. Box 65 - 00044 Frascati, (Rome) Italy

R. Giorgi, S. Martelli, S. Turtù, G. Zappa
ENEA, Area INN, Dip. PCM, C.R.E. Casaccia,
P.O.Box 2400 - 00100 Rome

ABSTRACT

Nanocrystalline Al_2O_3 powders were successfully synthesized by a CO_2 laser-driven gas-phase reaction involving trimethylaluminum ($\text{Al}(\text{CH}_3)_3$) and nitrous-oxide (N_2O). Ethylene (C_2H_4) was added as gas sensitizer. The as-synthesized powder particles showed a considerable carbon contamination and an amorphous-like structure. After thermal treatment at 1200-1400°C, the powder transformed to hexagonal α - Al_2O_3 with very low carbon contamination as confirmed by X-ray diffraction, X-ray photo-electron spectroscopy and chemical analysis. The calcinated powders resulted to be spherical single crystal nanoparticles with a mean size $\langle D \rangle$ of 15-20 nm, as determined by X-ray diffraction, electron microscopy and B.E.T. specific surface measurements. The laser synthesized Al_2O_3 particles are well suited dispersoids for intermetallic alloy technology.

INTRODUCTION

Intermetallic compounds, like NiAl and FeAl, are promising new materials for structural application, due to their high strength retention at elevated temperature combined with low density and good oxidation resistance. The breakthrough in intermetallic alloys technology has also opened up the possibility for improving the high temperature mechanical properties of this class of materials by introducing into the matrix, the major phase, a second minor phase. Second phase particles are able to harden the matrix by obstructing the dislocation motion. Oxide particles, like Al_2O_3 aluminium oxide, categorized as dispersoids are often synthetically added to enhance yield strength and creep resistance due to the mechanism of dispersion hardening [1]. The average size of the dispersoid particles is critical to the mechanical and metallurgical properties. According to Orowan's theory and its subsequent refinement [2], small dispersoid particles (1-100 nm) have the strongest effect on yield strength. The dispersoids should also be spherical in shape to minimize surface energy and they should exhibit a rather monodisperse distribution, since coarse dispersoids create problems of deformation compatibility and generate large stress gradients in their

vicinity.

The CO₂ laser-driven gas-phase synthesis method has already been successfully applied to produce silicon based nanoparticles [3-5]. In this process the reactant gases are heated by laser absorption in a small, well defined irradiation region having high temperature and very steep temperature gradients. The initial nucleation rate is very high and the subsequent particle growth is abruptly terminated as soon as the particles leave the hot zone. The produced particles are ultrafine, spherical, nearly monodispersed in size and extremely pure, since the chamber walls are cold and non reactive. Laser synthesis seems, therefore, well suited for producing oxide dispersoids. To our knowledge, Al₂O₃ nanopowders have never been produced by this method, so that this attempt is interesting both from a fundamental and technological point of view.

In this paper we present results on the CO₂ laser driven synthesis of nanosized Al₂O₃ powders starting from Al(CH₃)₃-trimethylaluminium (TMA) and N₂O-nitrous oxide as gas-phase reactants.

EXPERIMENTAL

The experimental set-up for laser synthesis has been described in details elsewhere [4,5]. In this experiment the CO₂ laser beam (maximum power = 1.2 kW) was focussed down to 3-4 mm at the centre of the reaction chamber, where it intersected the reactant effusive beam. The gas sensitizer (ethylene) was bubbled through liquid TMA acting, at the mean time, as TMA vapour carrier. The reactant gas mixture entered the cell through a 4 mm stainless steel nozzle. A coaxial Ar stream (1.5-2 l/m) was used to keep the nucleated particles entrained in the gas stream to the cell exit and to the collecting unit. The gas flow rates were independently controlled by flowmeters and the irradiated gaseous mixture composition was monitored by on-line mass spectrometry. The obtained powder have been characterized by X-ray diffraction (XRD), transmission electron microscopy (TEM), X-ray photoelectron spectroscopy (XPS) and B.E.T. specific surface measurement. The C content of the synthesized powder has been measured by the infrared absorption method after combustion in an induction furnace (HFIR). The oxygen analysis was carried out by inert gas fusion method employing a LECO apparatus R017. The Al content was determined by Inductively Coupled Plasma Atomic Emission Spectrometry (ICPAES).

RESULTS AND DISCUSSION

Al₂O₃ powders were synthesized by a CO₂ laser-driven gas-phase reaction involving TMA and N₂O. The choice of TMA as Al precursor was based on the well known suitability of metal alkyls as precursors for chemical vapour deposition (CVD) process due to their reasonable vapour pressure at room temperature (TMA vapour pressure = 9 mm Hg, at 20 °C) and to the low metal-carbon binding energy [6]. TMA reacts spontaneously with oxygen, thus it was necessary to find an oxygen donor molecule which can be dissociated only under laser irradiation. N₂O has been selected for its low dissociation energy [7] and to obtain the more reactive atomic oxygen instead of O₂ molecules. In order to activate the laser pyrolysis, C₂H₄ was chosen as sensitizer for its quasi resonant absorption at 10 μm and for having a dissociation energy (D(H₂C-CH₂) = 7.2 eV [7]) higher than N₂O (D(N₂-O) = 1.667 eV [7]) and Al(CH₃)₃ (D(Al-CH₃) = 2.9 eV [6]). The reactants are expected to dissociate after collisional energy transfer from vibrationally excited ethylene molecules.

All the parameters affecting the process, such as total pressure and gas flow rates in the cell, reactants and sensitizer relative concentrations and laser power, have been tuned up to optimize the powder productivity. A key role is played by

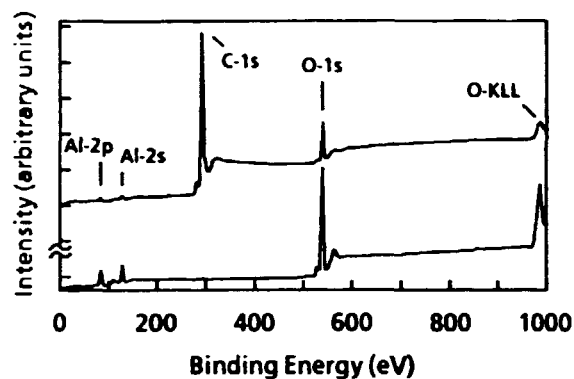


Fig. 1 XPS survey scans of (upper) as synthesized powder and (lower) 1200°C heat treated powder. The atomic Al/O ratios, as determined by quantitative XPS analysis, are 0.52 and 0.67 respectively (theoretical value: Al/O = 0.66).

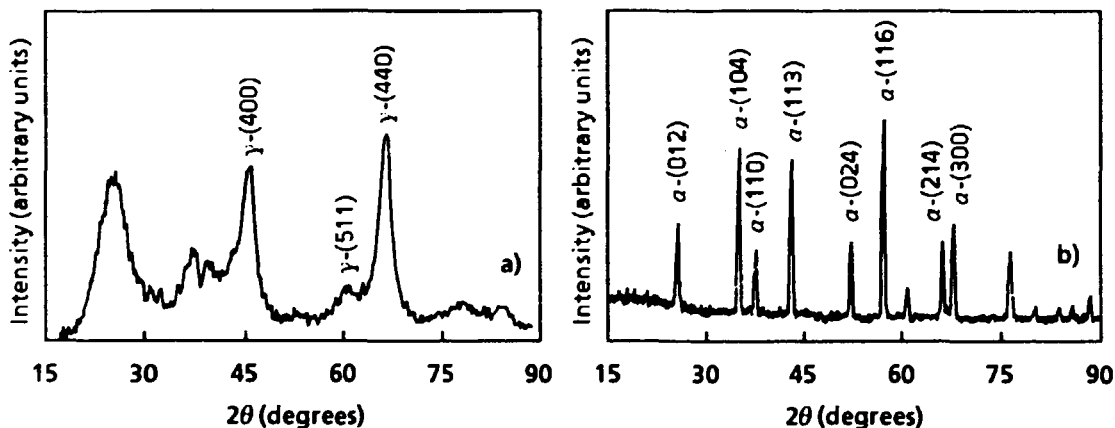
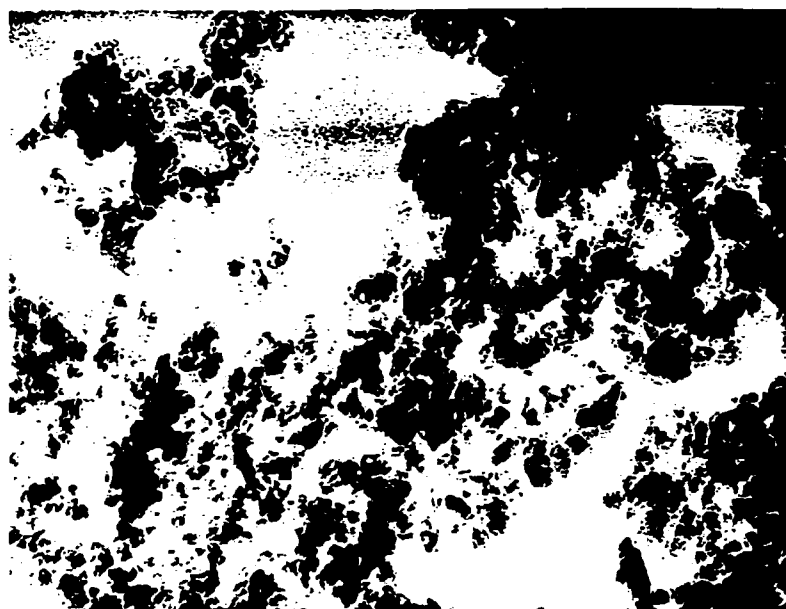


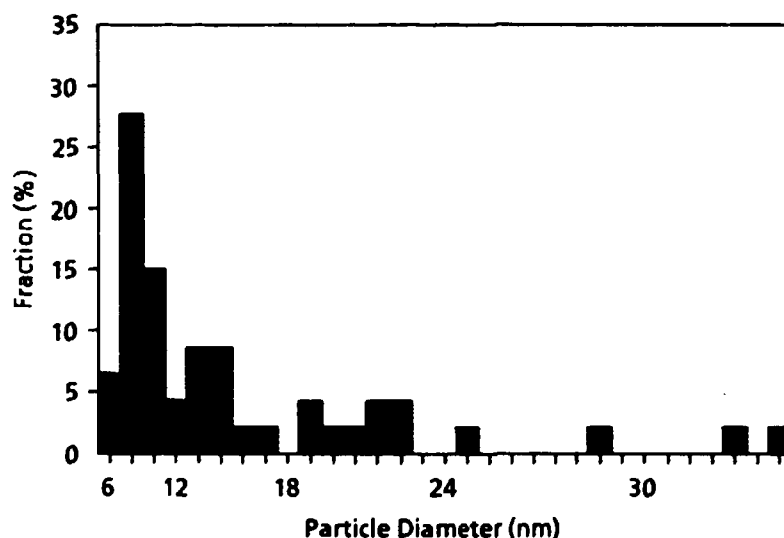
Fig. 2 X-ray $\text{CuK}\alpha$ diffraction pattern recorded in reflexion geometry: a) as synthesized powder; b) after thermal treatment at 1200°C.

ethylene because it carries the reactant gas (TMA) and absorbs the laser radiation, thus determining the energy transfer process and the reaction temperature. The ethylene flow rate and reaction chamber pressure were varied in order to maximize the flame temperature ($T_{\text{max}}=1270^\circ$) by keeping low the ethylene fragmentation, that is unavoidably increased by the addition of N_2O . The gas-phase product formation vs. the solid product yield was monitored by on-line mass spectrometry. It was found that in the absence of solid product, ethylene and TMA fragmentation is accompanied by an increase of the ion peaks corresponding to C-containing fragments. These ion peaks decrease as soon as solid product formation occurs, thus indicating that C containing fragments are incorporated in the powder. Ultrafine, dark powder is produced in a narrow range of process parameters and the maximum productivity (ca. 8 gr/hr) was observed with the following set of values: laser power 600 W, ethylene plus TMA flow rate=250 sccm, N_2O flow rate = 250 sccm, operating pressure= 53×10^3 P.

The chemical analysis of the as-synthesized powder put into evidence a very large carbon contamination (60 wt.%) while XPS-analysis showed a defective Al to O atomic ratio (Fig. 1). The XRD pattern, recorded on the as-synthesized powder



a)



b)

Fig. 3 a) TEM micrograph of Al_2O_3 particles after thermal treatment at 1200 °C. Bright field image. b) Particle size distribution determined from the dark field TEM micrograph of the same sample.

(Fig. 2a), presented broad interference peaks. Two main contributions have been distinguished: an amorphous component, indicated by the broad halo in the low angle part, and a highly disordered $\gamma\text{-Al}_2\text{O}_3$ form (JCPDS 29-63). The dimension of the coherent scattering domains (X-ray particle size) of the γ -form, calculated from the integral breadth of the (400) and (440) interference peaks [8], amounts to $\langle D \rangle_c = 3\text{-}4$ nm. To eliminate the carbon contamination, the powder has been thermally treated at temperatures ranging between 200 and 1400 °C, raising the temperature by 100 °C per hour. By heating up to 1000 °C, a considerable weight loss has been observed together with the change of colour to white. The chemical analysis confirmed the reduction of C powder content down to 0.2 ± 0.05 wt%. At the mean time XRD has not shown any appreciable structural change, suggesting a free carbon contamination of the as synthesized powder, probably originated by a partial cracking of ethylene. After the treatment at higher temperature (1200 °C) the hexagonal

structure of Al_2O_3 was established with a further decrement of carbon content to 0.05 ± 0.02 wt%. The whole XRD-pattern (Fig. 2b) can be thoroughly indexed as α - Al_2O_3 (Corundum, JCPDS 42-1468). XPS (Fig. 1) and chemical analysis confirm the low carbon content as well as the right stoichiometry of the thermally treated powder. No detectable difference was observed by increasing the temperature up to 1400 °C. The coherent scattering domain size, calculated from the integral breadth relative to the main diffraction peaks of the 1200 °C treated sample amounts to $\langle D \rangle_c = 15\text{-}20$ nm. The TEM micrograph of the same sample (Fig. 3a) shows spherical particles with a diameter distribution centred at about $\langle D \rangle_T = 15$ nm (Fig. 3b). B.E.T measurement gave a value of $70 \text{ m}^2/\text{g}$ for the specific surface of this sample. Assuming a spherical shape of the powder particles and a mass density $\rho = 3.89 \text{ g/cm}^3$ (α - Al_2O_3) a mean particle diameter $\langle D \rangle_B = 21$ nm can be estimated. Even though TEM micrographs are not statistically significant, the good agreement between the $\langle D \rangle_B$ and $\langle D \rangle_T$ values assures a narrow particle size distribution. Moreover the equivalence of the physical dimension and of the coherence size suggests, that each powder particle is a quite perfect Al_2O_3 nanosized single crystal, since the apparent X-ray size is strongly affected by the presence of lattice defects [8]. In conclusion it has been proved, that laser assisted synthesis can be applied to produce Al_2O_3 ultrafine particle from gaseous precursors. The Al_2O_3 particles fulfil perfectly the requirement for oxide dispersion strengthening, as it concerns mean size, particle distribution, shape and chemical purity.

The authors wish to thank Mr. R. Belardinelli for his precious technical assistance during the experimental work.

REFERENCES

- [1] A. U. Seybolt, "Oxide Dispersion-Strengthened NiAl and FeAl", Trans. of the ASM, 59, 860 (1966);
- [2] J. L. Strudel, "Mechanical Properties of Multiphase Alloys" in Physical Metallurgy, 3rd edition, ed. by R. W. Cahn and P. Haasen, (North Holland 1983), p. 1415;
- [3] R. Fantoni, E. Borsella, S. Piccirillo, R. Ceccato and S. Enzo, "Laser Synthesis and Characterization of Ultrafine Powders" J. Mater. Res., 5, 143 (1990);
- [5] E. Borsella, S. Botti, R. Fantoni, R. I. Morjan, C. Popescu, T. Dikonimos-Makris, R. Giorgi and S. Enzo, "Composite Si/C/N Powder Production by laser Induced Gas-Phase Reactions", J. Mater. Res., 7, 2257 (1992);
- [6] G. Pilcher, H. A. Skinner in "The Chemistry of the Metal-Carbon Bond" ed. by F.R. Hartley and S. Patai (Wiley, N. Y. 1982) Vol.1, p. 69;
- [7] G. Herzberg "Molecular Spectra and Molecular Structure", Vol.III (Van Nostrand-Reinold, N.Y. 1966);
- [8] A. Guinier "Théorie et Technique de la Radiocristallographie" (Dunod, Paris 1964) 62.



MICROCOPY RESOLUTION TEST CHART
NATIONAL BUREAU OF STANDARDS
STANDARD REFERENCE MATERIAL 1010a
(ANSI and ISO TEST CHART No. 2)